

## Identification and Characterization of Novel Benzil (Diphenylethane-1,2-dione) Analogues as Inhibitors of Mammalian Carboxylesterases

Randy M. Wadkins,<sup>†</sup> Janice L. Hyatt,<sup>‡</sup> Xin Wei,<sup>‡</sup> Kyoung Jin P. Yoon,<sup>‡</sup> Monika Wierdl,<sup>‡</sup> Carol C. Edwards,<sup>‡</sup> Christopher L. Morton,<sup>‡</sup> John C. Obenauer,<sup>§</sup> Komath Damodaran,<sup>#</sup> Paul Beroza,<sup>#</sup> Mary K. Danks,<sup>‡</sup> and Philip M. Potter<sup>\*,‡</sup>

Department of Chemistry and Biochemistry, University of Mississippi, University, Mississippi 38677, Department of Molecular Pharmacology and Hartwell Center for Bioinformatics and Biotechnology, St. Jude Children's Research Hospital, Memphis, Tennessee 38105, and Telik Inc., Palo Alto, California 94304

Received December 3, 2004

Carboxylesterases (CE) are ubiquitous enzymes responsible for the metabolism of xenobiotics. Because the structural and amino acid homology among esterases of different classes, the identification of selective inhibitors of these proteins has proved problematic. Using Telik's target-related affinity profiling (TRAP) technology, we have identified a class of compounds based on benzil (1,2-diphenylethane-1,2-dione) that are potent CE inhibitors, with  $K_i$  values in the low nanomolar range. Benzil and 30 analogues demonstrated selective inhibition of CEs, with no inhibitory activity toward human acetylcholinesterase or butyrylcholinesterase. Analysis of structurally related compounds indicated that the ethane-1,2-dione moiety was essential for enzyme inhibition and that potency was dependent on the presence of, and substitution within, the benzene ring. 3D-QSAR analyses of these benzil analogues for three different mammalian CEs demonstrated excellent correlations of observed versus predicted  $K_i$  ( $r^2 > 0.91$ ), with cross-validation coefficients ( $q^2$ ) of 0.9. Overall, these results suggest that selective inhibitors of CEs with potential for use in clinical applications can be designed.

### Introduction

The enzymatic detoxification of xenobiotics in both prokaryotes and eukaryotes is achieved in part by CEs.<sup>1</sup> These enzymes are ubiquitous and are expressed in tissues such as the lung, liver, kidney, and intestine that are exposed to chemicals or toxins. CEs metabolize many ester-containing compounds including heroin, cocaine, procaine, CPT-11 (irinotecan, 7-ethyl-10-[4-(1-piperidino)-1-piperidino]carbonyloxycamptothecin), capecitabine, and mivacurium (see refs 1–4 and references therein). The enzymes can also act as suicide substrates for organophosphate poisons, providing protection from agents such as sarin, soman, and tabun.<sup>5</sup>

Recently, the X-ray crystal structures of a rabbit CE (rCE) and a human liver CE (hCE1) have been determined,<sup>6–8</sup> and the proteins demonstrate significant structural homology to other classes of esterases, particularly acetylcholinesterases (AcChE) and lipases. Indeed, the rCE and hCE1 structures are highly homologous, with only  $\sim 1.0$  Å rmsd variation over 455 residues of the  $\alpha$ -carbon trace,<sup>7,8</sup> consistent with the amino acid sequences that are greater than 81% identical. However, despite this apparent structural similarity, significant differences in substrate specificity exist. For example, rCE catalyzes the hydrolysis of CPT-11

to SN-38 (7-ethyl-10-hydroxycamptothecin), whereas hCE1 is approximately 100- to 1000-fold less efficient at this reaction.<sup>9,10</sup>

Because of the high degree of similarity among the esterases, reports detailing the identification of selective inhibitors of CEs have been limited. Of those that have been identified, the structures are typically based on either organophosphate compounds such as bomin or trifluoromethyl ketone (TFK) analogues as described by Wheelock et al.<sup>11,12</sup> It would be expected that both classes of compounds would be readily hydrolyzed by water. In fact, the TFK-containing compounds were reported to be hygroscopic, thereby hampering efforts to develop these compounds for use in clinical applications.

Our goal, therefore, was to identify nontoxic selective CE inhibitors that might have applications in either the prevention of drug toxicity (e.g., by inhibiting morphine production from heroin) or increasing the half-life of drugs that are inactivated by CEs. Such drugs include fleistolol, a  $\beta$ -adrenergic blocking agent, which has a dramatically reduced half-life in vivo due to CE-mediated hydrolysis.<sup>13</sup> By administration of a specific inhibitor in combination with the drug of choice, prolonged plasma concentrations and hence greater efficacy might be achieved. To identify such inhibitors, we applied Telik's lead technology TRAP (target-related affinity profiling).<sup>14–16</sup> Using this approach, we identified an analogue of benzil that selectively inhibited a variety of CEs. Following analysis of over 31 benzil analogues, we have developed QSAR models for the inhibition of rCE, hCE1, and a human intestinal CE (hiCE, hCE2).

\* To whom correspondence should be addressed. Phone: 901-495-3440. Fax: 901-521-1668. E-mail: phil.potter@stjude.org.

<sup>†</sup> University of Mississippi.

<sup>‡</sup> Department of Molecular Pharmacology, St. Jude Children's Research Hospital.

<sup>§</sup> Hartwell Center for Bioinformatics and Biotechnology, St. Jude Children's Research Hospital.

<sup>#</sup> Telik Inc.

These analogues do not inhibit human acetylcholinesterase (hAcChE) or butyrylcholinesterase (hBuChE) but are potent inhibitors of mammalian CEs, with  $K_i$  values in the low nanomolar range.

## Experimental Section

**Chemicals.** Compounds were purchased from the following sources. Benzil (**1**), **3–7**, **14**, **19**, **20**, **22–26**, **28**, **31**, **36**, **38–40**, **53**, **57–59**, and **61** were all purchased from Sigma Aldrich Biochemicals (St. Louis, MO). **2**, **18**, **21**, **48**, and **49** were obtained from Pfaltz and Bauer (Waterbury, CT). **8**, **11**, **15**, **43–47**, **50–52**, and **56** were purchased from Alfa Aesar (Ward Hill, MA). **10**, **41**, and **60** were obtained from VWR Scientific Products (West Chester, PA). **16** was purchased from Ryan Scientific (Isle of Palms, SC). **17** was obtained from Toronto Research Chemicals (Toronto, Canada). **27**, **32**, and **35** were purchased from Maybridge (Tintagel, U.K.). **29**, **30**, **33**, and **34** were obtained from Industrial Research Ltd., (Auckland, New Zealand). **37** and **54** were purchased from TCI America (Portland, Oregon), and **42** and **55** were obtained from ACROS (Fisher Scientific, Pittsburgh, PA). The synthesis of compounds **9**, **12**, and **13** is described in this article.

CPT-11 was kindly provided by Dr. J. P. McGovren (Pfizer, Cambridge, MA).

**Synthetic Reagents.** 4-Chlorobenzaldehyde, 3,5-difluorobenzaldehyde, 3,4,5-trifluorobenzaldehyde, thiamine, copper acetate, and ammonium nitrate were all purchased from Sigma Aldrich.

**Enzymes.** Pure rCE and hCE1 were prepared as described previously.<sup>17</sup> hiCE was prepared by concentration of baculovirus media from Sf9 cells expressing a secreted form of the protein. While not homogeneous, the preparation was at least 60% pure. Since no CE activity is expressed or secreted from uninfected Sf9 cells, the only CE present in the culture media was the recombinant protein. The Genbank accession numbers for the cDNAs used for CE production were as follows: rCE, AF036930;<sup>18</sup> hCE1, M73499;<sup>19</sup> hiCE, Y09616.<sup>20</sup>

Human AcChE and BuChE were obtained from Sigma Aldrich.

**Library of Compounds and TRAP Screening.** Screening of compounds was performed using a library of small molecules obtained from Telik using their target-related affinity profiling (TRAP) technology.<sup>15</sup> Briefly, TRAP defines an “affinity fingerprint” for a particular molecule by determining its binding affinities to a panel of proteins. In an iterative screening process (~70 compounds for each iteration), computational analysis of fingerprints is performed and compared to the biological activity obtained for each compound. The first series of compounds to be assayed was chosen because their fingerprints encompassed the diversity of fingerprints present within the entire library. Subsequent analyses are based on computational analysis of the fingerprints of the compounds that inhibited CEs. Routinely three to four iterations were performed using approximately 300 compounds. The advantage of this methodology is that molecules of multiple chemotypes demonstrating inhibitory activity can be identified by assaying as few as 200 compounds.<sup>14,15</sup>

**Enzyme Inhibition Assays and Determination of  $K_i$  Values Using Nitrophenyl Acetate (*o*-NPA) as a Substrate.** CE inhibition was determined using a spectrophotometric multiwell plate assay with 3mM *o*-NPA as a substrate.<sup>18,21</sup> Briefly, test compound (100  $\mu$ M) and substrate were aliquoted into wells and enzyme was added using a multiwell pipettor. The rate of change in absorbance at 420 nm was measured at 15 s intervals for 5 min and compared to wells containing no inhibitor. Compounds that demonstrated 50% reduction in CE activity were subsequently evaluated in detail. Routinely, assays were performed in duplicate and included both positive (50  $\mu$ M bis(4-nitrophenyl) phosphate (BNPP)) and negative controls (DMSO, no enzyme).

Further analysis of inhibitors was performed in a similar fashion except that inhibitor concentrations ranged from 1 pM

to 100  $\mu$ M, and data were fitted to the following equation to determine the mode of enzyme inhibition:<sup>22</sup>

$$i = \frac{[I]\{[s](1 - \beta) + K_s(\alpha - \beta)\}}{[I]\{[s] + \alpha K_s\} + K_i\{\alpha[s] + \alpha K_s\}}$$

where  $i$  is the fractional inhibition,  $[I]$  is the inhibitor concentration,  $[s]$  is the substrate concentration,  $\alpha$  is the change in affinity of substrate for enzyme,  $\beta$  is the change in the rate of enzyme substrate complex decomposition,  $K_s$  is the dissociation constant for the enzyme substrate complex, and  $K_i$  is the inhibitor constant. Examination of the curve fits where  $\alpha$  ranged from 0 to  $\infty$  and  $\beta$  ranged from 0 to 1 was performed using GraphPad Prism software and Perl data language. The curves generating the highest  $r^2$  values were analyzed using Akaike's information criteria<sup>23,24</sup> to identify the best model for enzyme inhibition.  $K_i$  values were then calculated from the equation predicted by Prism to be the best fit for the experimental data.

**Enzyme Inhibition Assays Using 4-Methylumbelliferone Acetate (4-MUA) as a Substrate.** Metabolism of 4-MUA was assessed by a fluorimetric assay using either a Hitachi F2000 fluorescence spectrophotometer or a Millipore Cytofluor 2350 with an excitation wavelength of 365 nm and an emission wavelength of 460 nm. Samples were incubated with 0.75 mM of 4-MUA in 50 mM Hepes, pH7.4, and the release of 4-methylumbelliferone was measured over a 1 min time interval. The rate of substrate catalysis was linear over this time period. Enzyme inhibition by selected compounds and determination of  $K_i$  values were performed as described above.

**Inhibition of Acetylcholinesterase and Butyrylcholinesterase.** The ability of compounds to inhibit hAcChE and hBuChE was performed as previously described using either 1 mM acetylthiocholine (AcTCh) or 1 mM butyrylthiocholine (BuTCh), respectively, as substrates.<sup>25–28</sup>

**Synthesis of Benzil Analogues.** Benzil analogues were synthesized by condensation of the substituted benzaldehydes (0.04 mol) in the presence of thiamine hydrochloride (0.002 mol) and alcoholic sodium hydroxide (0.005 mol) to yield the benzoin,<sup>29</sup> with subsequent oxidation using copper acetate (0.001 mol) and ammonium nitrate (0.006 mol) in 80% acetic acid.<sup>30</sup> Products were purified by recrystallization, melting points were determined using a Mel-temp (Barnstead International, Dubuque, IA), and purity and structures were assessed by TLC, NMR, and total C, H, N analysis.

**4,4'-Dichlorobenzil (1,2-Bis(4-chlorophenyl)ethane-1,2-dione, **9**).** 4,4'-Dichlorobenzil was synthesized from 1,2-bis-(4-chlorophenyl)-2-hydroxyethanone to yield a yellow solid (yield 62%). Physical and NMR parameters of **9** were as follows: mp 196–198 °C; <sup>1</sup>H NMR (500 MHz, CDCl<sub>3</sub>)  $\delta$  7.53 (d, 2H,  $J$  = 8.5 Hz, Ar-*H*), 7.94 (d, 2H,  $J$  = 8.5 Hz, Ar-*H*).

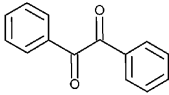
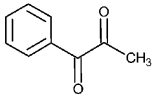
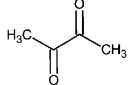
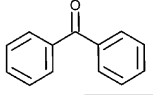
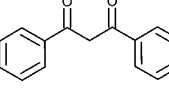
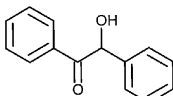
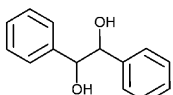
**1,2-Bis(3,5-difluorophenyl)ethane-1,2-dione (**12**).** 1,2-Bis(3,5-difluorophenyl)ethane-1,2-dione was synthesized from 1,2-bis(3,5-difluorophenyl)-2-hydroxyethanone to yield a yellow solid (yield 74%). Physical and NMR parameters of **12** were as follows: mp 135–137 °C; <sup>1</sup>H NMR (500 MHz, CDCl<sub>3</sub>)  $\delta$  7.15 (dd, 2H,  $J$  = 2.4 Hz, Ar-*H*), 7.51 (dt, 4H,  $J$  = 2.2 Hz, Ar-*H*).

**1,2-Bis(3,4,5-trifluorophenyl)ethane-1,2-dione (**13**).** 1,2-Bis(3,4,5-trifluorophenyl)ethane-1,2-dione was synthesized from 2-hydroxy-1,2-bis(3,4,5-trifluorophenyl)ethanone to yield a yellow solid (yield 96%). Physical and NMR parameters of **13** were as follows: mp 102–103 °C; <sup>1</sup>H NMR (500 MHz, CDCl<sub>3</sub>)  $\delta$  7.68 (d, 4H,  $J$  = 6.6 Hz, Ar-*H*).

**Irreversible Enzyme Inhibition Assays.** Irreversible inhibition of CEs by the inhibitors was assessed by preincubating the enzymes with the compounds at 1  $\mu$ M on ice for either 1 or 24 h. After incubation, the samples were extensively diluted in 50 mM Hepes, pH7.4, and CE activity was determined using 3mM *o*-NPA as a substrate. As a positive control, 50  $\mu$ M BNPP was included in these assays.

**Molecular Modeling of Benzil-Based Carboxylesterase Inhibitors.** 3D-QSAR analyses were performed using Quasar 4.0<sup>31,32</sup> running on a Macintosh G4. Structures for each analogue were initially constructed with ChemBats3D for

**Table 1.**  $K_i$  Values for the Inhibition of CEs by Benzil and Related Compounds<sup>a</sup>

ID	Name	Structure	$K_i$ (nM) $\pm$ SE			
			hiCE	hCE1	rCE	hAcChE
1	Benzil		14.7 $\pm$ 1.9	45.1 $\pm$ 3.2	103 $\pm$ 19	>100,000
2	1-Phenylpropane-1,2-dione		1,840 $\pm$ 260	5,270 $\pm$ 1,730	4,930 $\pm$ 1,320	>100,000
3	Butan-2,3-dione		>100,000	>100,000	>100,000	>100,000
4	Benzophenone		>100,000	>100,000	>100,000	>100,000
5	1,3-Diphenylpropane-1,3-dione		>100,000	26,000 $\pm$ 1,880	3,950 $\pm$ 970	>100,000
6	Benzoin		2,220 $\pm$ 460	7,250 $\pm$ 2,370	>100,000	>100,000
7	1,2-Diphenylethane-1,2-diol		>100,000	>100,000	>100,000	>100,000

<sup>a</sup> Values for CEs were determined using *o*-NPA as a substrate, and those for hAcChE were determined using AcTCh as a substrate.

Macintosh. Partial atomic charges from the bond charge correction method<sup>33</sup> and AMBER atom types were assigned using the *antechamber* module of AMBER7 (University of California, San Francisco, CA). Structures for QSAR analysis were performed by initial energy minimization of benzil using the AM1 Hamiltonian of MOPAC.<sup>34</sup> The final structure was in excellent agreement with the structure obtained from higher level molecular orbital calculations and experimental data.<sup>35</sup> All benzil derivatives were then modeled from this minimized structure and individually minimized to remove steric conflicts.

The Quasar program produces a 3D receptor-surface model containing information about the molecular properties of both the ligand and the docking site. Essentially the software constructs pseudoreceptor models by positioning points of charge at vertexes around the pharmacophore under examination. These vertexes had charges of +0.1e, +0.5e, 0.0e, -0.1e, or -0.5e. Initially, a population of 200 models was generated for each enzyme inhibition data set and evaluated via a genetic algorithm to produce approximately 7000 new pseudoreceptor models. Evaluation of these models was then performed until the cross-validated correlation coefficient ( $q^2$ ) reached  $\geq 0.9$  for predicted vs experimental  $K_i$  values for each CE. Under these conditions, correlation coefficients ( $r^2$ ) for the predicted vs experimental  $K_i$  data were linear ( $>0.91$ ) for each enzyme model.

**Quantitation of CPT-11 and SN-38.** CPT-11 and SN-38 concentrations were determined using an HPLC-based assay with a fluorescent detector as previously described.<sup>9,36</sup>

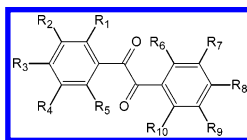
## Results

**Identification of Benzil as a General Carboxyl-esterases Inhibitor.** The identification of the benzil chemotype as a general inhibitor of CEs was the result of a directed screen using Telik's TRAP technol-

ogy.<sup>14,15,37,38</sup> Briefly, 70–80 compounds were screened for inhibition of *o*-NPA metabolism by each CE, and the initial set of compounds was chosen from the library because they represented the diversity of the entire compound collection. The screening process is iterative: the initial set of compounds to screen is chosen for the diversity of its general protein binding characteristics; subsequent sets are chosen on the basis of computational analysis of hits identified in earlier iterations.<sup>14</sup> This process allowed the identification of bona fide potent CE inhibitors with as few as 230 assays. These data indicated that benzil was a potent inhibitor of hiCE, hCE1, and rCE but demonstrated no inhibition of hAcChE.

Having identified benzil (see Table 1) as a general inhibitor of mammalian CEs, we assessed the ability of analogues having similar structures to this compound to inhibit catalysis of *o*-NPA by CEs. Table 1 indicates the  $K_i$  values for benzil and a series of structurally related agents. Replacement of either or both of the carbonyl chemotypes with hydroxyl moieties resulted in loss of enzyme inhibition. Similarly, removal of one carbonyl group as in benzophenone (**4**) or increasing the spacing between the diones as in 1,3-diphenylpropane-1,3-dione (**5**) resulted in compounds that were unable to inhibit CE-mediated catalysis of *o*-NPA. Finally, replacement of the benzene rings with methyl groups increased the  $K_i$  values of the inhibitors from 47- to 6800-fold. For example, with hCE1 the  $K_i$  values for benzil (**1**), 1-phenylpropane-1,2-dione (**2**), and butan-2,3-



**Table 2.** Structure of Benzil-Based Carboxylesterase Inhibitors<sup>a</sup>

compd	name	R1	R2	R3	R4	R5	R6	R7	R8	R9	R10
1	benzil (diphenylethane-1,2-dione)										
8	4,4'-difluorobenzil (1,2-bis(4-fluorophenyl)ethane-1,2-dione)			F					F		
9	4,4'-dichlorobenzil (1,2-bis(4-chlorophenyl)ethane-1,2-dione)			Cl					Cl		
10	2,2'-dichlorobenzil (1,2-bis(2-chlorophenyl)ethane-1,2-dione)	Cl					Cl				
11	4,4'-dibromobenzil (1,2-bis(4-bromophenyl)ethane-1,2-dione)			Br					Br		
12	1,2-bis(3,5-difluorophenyl)ethane-1,2-dione		F		F			F		F	
13	1,2-bis(3,4,5-trifluorophenyl)ethane-1,2-dione		F	F	F			F	F	F	
14	4-[oxo(phenyl)acetyl]benzoic acid								COOH		
15	1-(4-chlorophenyl)-2-phenylethane-1,2-dione								Cl		
16	1-(4-chlorophenyl)-2-(4-methylphenyl)ethane-1,2-dione			CH <sub>3</sub>					Cl		
17	1-(4-methylphenyl)-2-phenylethane-1,2-dione								CH <sub>3</sub>		
18	1,2-bis(4-methylphenyl)ethane-1,2-dione			CH <sub>3</sub>					CH <sub>3</sub>		
19	1-(3,4-dimethylphenyl)-2-phenylethane-1,2-dione							CH <sub>3</sub>	CH <sub>3</sub>		
20	1-(4-methoxyphenyl)-2-phenylethane-1,2-dione								OCH <sub>3</sub>		
21	1,2-bis(4-methoxyphenyl)ethane-1,2-dione			OCH <sub>3</sub>					OCH <sub>3</sub>		
22	1,2-bis(3-methoxyphenyl)ethane-1,2-dione				OCH <sub>3</sub>						OCH <sub>3</sub>
23	1-(2-chlorophenyl)-2-(3,4-dimethoxyphenyl)ethane-1,2-dione	Cl						OCH <sub>3</sub>	OCH <sub>3</sub>		
24	1-[4-(bromomethyl)phenyl]-2-phenylethane-1,2-dione			Br				NO <sub>2</sub>	Br		
25	1,2-bis(4-bromo-3-nitrophenyl)ethane-1,2-dione				NO <sub>2</sub>			NO <sub>2</sub>	CH <sub>3</sub>		
26	1-(4-methyl-3-nitrophenyl)-2-phenylethane-1,2-dione							NO <sub>2</sub>	NO <sub>2</sub>		
27	1-(4-nitrophenyl)-2-phenylethane-1,2-dione								NO <sub>2</sub>		
28	1-(2,4-dinitrophenyl)-2-phenylethane-1,2-dione						NO <sub>2</sub>		NO <sub>2</sub>		
29	1,2-bis(3-nitrophenyl)ethane-1,2-dione		NO <sub>2</sub>					NO <sub>2</sub>			
30	1,2-bis(4-hydroxyphenyl)ethane-1,2-dione			OH					OH		
31	1,2-bis(5-bromo-2-hydroxyphenyl)ethane-1,2-dione	OH			Br		OH			Br	
32	1,2-bis(2,4-dihydroxyphenyl)ethane-1,2-dione	OH		OH			OH		OH		
33	1,2-bis(4-hydroxy-3-nitrophenyl)ethane-1,2-dione		NO <sub>2</sub>	OH				NO <sub>2</sub>	OH		
34	1,2-bis(4-methoxy-3-nitrophenyl)ethane-1,2-dione		NO <sub>2</sub>	OCH <sub>3</sub>				NO <sub>2</sub>	OCH <sub>3</sub>		
35	1,2-bis[4(dimethylamino)phenyl]ethane-1,2-dione			(CH <sub>3</sub> ) <sub>2</sub> N					(CH <sub>3</sub> ) <sub>2</sub> N		
36	1-(pentachlorophenyl)-2-(pentafluorophenyl)ethane-1,2-dione	Cl	Cl	Cl	Cl	Cl	F	F	F	F	F
37	1-[4-[oxo(phenyl)acetyl]phenyl]-2-phenylethane-1,2-dione								COCOC <sub>6</sub> H <sub>5</sub>		

<sup>a</sup> R = H unless otherwise indicated.

dione (**3**) were 45, 5270, and greater than 100 000 nM, respectively. Overall, these results suggest that the 1,2-dione structure is essential for enzyme inhibition and that increased potency toward CEs is provided by the phenyl rings.

**Analysis of CE Inhibition by Benzil Analogues.** The TRAP screen identified the key structural components that were required for CE inhibition (e.g., 1,2-dione, aromatic moieties). We then tested commercially available agents having these characteristics (see Tables 2, 3, 4, and 5) for their ability to inhibit the CEs, hiCE, hCE1, and rCE, as well as hAcChE and hBuChE. As indicated in Table 4, a wide range of  $K_i$  values for the inhibition of CE-mediated catalysis of *o*-NPA was observed for various benzil analogues. None of these agents inhibited hAcChE or hBuChE at concentrations up to 100  $\mu$ M.

In general, the inhibitors fell into two distinct classes: those that inhibited all three CEs (e.g., benzil (**1**), **15**, and **37**) and those that only inhibited hiCE and rCE (e.g., compounds **21**, **28**, and **31**). A general correlation between the size of the inhibitor and the ability to inhibit CEs was observed such that the larger compounds inhibited both rCE and hiCE and the smallest molecules inhibited all three CEs.

**Assessment of the Mode of CE Inhibition by Benzil.** Analysis of the curve fits obtained using the equation described by Webb<sup>22</sup> suggested that the mode of enzyme inhibition for benzil and its analogues was

partially competitive. Hence, while benzil and its analogues acted in a competitive fashion, at infinite concentrations of inhibitor the reaction velocity was not reduced to zero. This observation suggests that the compounds act as inhibitors because they demonstrate similarity to bona fide enzyme substrates. To determine whether benzil and several selected analogues could produce irreversible inhibition of CEs, we determined the ability of the enzymes to metabolize *o*-NPA after preincubation with the inhibitors. As indicated in Figure 1, no irreversible inhibition was observed with benzil or any of the analogues tested. In contrast, greater than 95% inhibition was observed using BNPP, an inhibitor known to irreversibly bind to and inactivate esterases.

**QSAR Analysis of Benzil-Mediated CE Inhibition.** 3D-QSAR analysis of the inhibition data was performed using Quasar 4.0 (Figure 2), and Table 6 indicates the correlation coefficients ( $r^2$  values) for the experimental versus predicted  $K_i$  values. As indicated, these coefficients are close to unity (0.919–0.925), suggesting that the models provide an accurate estimation of the inhibition constants. In addition, the  $q^2$  values (the cross-correlation coefficients) for all of the models were 0.90. Since  $q^2$  correlations of greater than 0.4 are considered adequate for QSAR modeling of biological data,<sup>39</sup> these results indicate that these models should be suitable for future inhibitor design.

Graphic representations of the 3D-QSAR models for hiCE, hCE1, and rCE are depicted in Figure 3. Benzil

**Table 3.** Names and Structures of Additional Compounds Tested for CE Inhibition

ID	Name	Structure
2	1-Phenylpropane-1,2-dione	
3	Butane-2,3-dione	
4	Benzophenone	
5	1,3-Diphenylpropane-1,3-dione	
6	Benzoin (2-hydroxy-1,2-diphenylethanone)	
7	1,2-Diphenylethane-1,2-diol	
38	Anisoin (2-hydroxy-1,2-bis(4-methoxyphenyl)ethanone)	
39	2-[4-(Dimethylamino)phenyl]-2-hydroxy-1-phenylethanone	
40	4-Benzoylbenzoic acid	
41	1-Phenylpentane-1,4-dione	
42	2,2-dimethoxy-1,2-diphenylethanone	
43	Pentane-2,3-dione	
44	Pentane-2,4-dione	
45	3-Methylcyclopentane-1,2-dione	
46	3-Methylcyclopentane-1,3-dione	
47	Heptane-2,3-dione	
48	Cyclohexane-1,2-dione	
49	Cyclohexane-1,3-dione	
50	3-Methylcyclohexane-1,2-dione	
51	2-Methylcyclohexane-1,3-dione	
52	3,5,5-Trimethylcyclohexane-1,2-dione	
53	1,4-Benzoquinone	
54	3,5-di(tert-butyl)-1,2-benzoquinone	
55	Tetrachloro-1,2-quinone	
56	Tetrachloro-1,4-quinone	
57	5,6-Dimethylmorpholine-2,3-dione	
58	6,7-Dichloroquinoxaline-2,3-dione	
59	Benzyl sulfone	
60	Benzyl phenyl sulfone	
61	Dibenzyl sulfoxide	

was positioned in the enzyme active site as shown, with the colored amino acid residues determined from our previous homology models of hiCE, hCE1, and rCE.<sup>38</sup> No simple descriptor of the active site gorge would explain the inhibitory activity of the benzils toward each enzyme. Rather, it is the overall hydrophobic and electrostatic milieu of the binding site that contributes to the affinity of each benzil, and these characteristics are slightly different for each enzyme.

It is noted that even though the pseudoreceptor model was derived completely independently of any protein structure, the correlation between the locations of the amino acids and charged areas in the pseudoreceptor model is quite striking. These correlations are in part validated by the  $r^2$  and  $q^2$  values as indicated in Table 6.

**Inhibition of CE-Mediated Metabolism of 4-Methylumbelliferone Acetate and CPT-11.** Since benzil and its analogues act as partially competitive inhibitors of CEs, we assessed the ability of several compounds to inhibit the metabolism of 4-MUA and the anticancer drug CPT-11. As indicated in Table 7, the benzil analogues were potent inhibitors of metabolism

of all substrates, with  $K_i$  values ranging from 0.029 to 175 nM. As expected, there were differences in the ability of each compound to inhibit the metabolism of the ester substrates. For example, with 4,4'-dibromobenzil (**11**), this inhibitor was highly effective at preventing metabolism of 4-MUA with all three mammalian CEs; however, **11** did not inhibit *o*-NPA or CPT-11 metabolism by hiCE. Interestingly, the dichloro derivative (4,4'-dichlorobenzil, **9**) was a good inhibitor of rCE and hCE1 with *o*-NPA, CPT-11, or 4-MUA but not with CPT-11 with hiCE, suggesting that the halogen atom present at the 4 and 4' positions of the molecule significantly affects specificity with respect to both enzyme and substrate. It is apparent that the benzil analogues are potent inhibitors of CE-mediated metabolism of different esterase substrates and that they act in a partially competitive fashion.

## Discussion

We have identified benzil as a potent selective inhibitor of hCE1, hiCE, and rCE.  $K_i$  values for this compound and related analogues ranged from 4 nM to 18  $\mu$ M for the mammalian CEs. More importantly, these agents

**Table 4.**  $K_i$  Values for hiCE, hCE1, rCE, and hAcChE with the Benzil Analogues<sup>a</sup>

compd	hiCE $K_i \pm SE$ (nM)	hCE1 $K_i \pm SE$ (nM)	rCE $K_i \pm SE$ (nM)	hAcChE $K_i$ (nM)	hBuChE $K_i$ (nM)
1	14.7 $\pm$ 1.9	45.1 $\pm$ 3.2	103 $\pm$ 19	>100 000	>100 000
8	167 $\pm$ 12	231 $\pm$ 12	398 $\pm$ 59	>100 000	>100 000
9	106 $\pm$ 22	182 $\pm$ 21	9.5 $\pm$ 1.5	>100 000	>100 000
10	353 $\pm$ 62	1650 $\pm$ 300	220 $\pm$ 37	>100 000	>100 000
11	>100 000	>100 000	4.1 $\pm$ 0.5	>100 000	>100 000
12	23.4 $\pm$ 3.6	73.5 $\pm$ 8.4	17.5 $\pm$ 2.7	>100 000	>100 000
13	259 $\pm$ 53	372 $\pm$ 99	47.9 $\pm$ 18	>100 000	>100 000
14	71.5 $\pm$ 10	524 $\pm$ 46	64.0 $\pm$ 6.2	>100 000	>100 000
15	18.2 $\pm$ 3.6	47.4 $\pm$ 6.8	23.9 $\pm$ 2.9	>100 000	>100 000
16	22.8 $\pm$ 3.9	160 $\pm$ 32	16.2 $\pm$ 1.7	>100 000	>100 000
17	33.3 $\pm$ 6.0	125 $\pm$ 15	119 $\pm$ 20	>100 000	>100 000
18	60.4 $\pm$ 6.0	532 $\pm$ 35	49.6 $\pm$ 6.8	>100 000	>100 000
19	4.1 $\pm$ 0.4	99.1 $\pm$ 10	108 $\pm$ 8.8	>100 000	>100 000
20	10.3 $\pm$ 0.6	175 $\pm$ 8.5	200 $\pm$ 60	>100 000	>100 000
21	70.2 $\pm$ 1.1	3410 $\pm$ 550	580 $\pm$ 160	>100 000	>100 000
22	139 $\pm$ 20	1540 $\pm$ 320	72.1 $\pm$ 9.1	>100 000	>100 000
23	8.9 $\pm$ 0.9	3300 $\pm$ 560	36.0 $\pm$ 12	>100 000	>100 000
24	21.3 $\pm$ 1.4	77.6 $\pm$ 5.5	15.0 $\pm$ 1.6	>100 000	>100 000
25	>100 000	>100 000	8.7 $\pm$ 1.3	>100 000	>100 000
26	7.9 $\pm$ 1.0	295 $\pm$ 9.6	11.9 $\pm$ 1.1	>100 000	>100 000
27	30.6 $\pm$ 5.0	215 $\pm$ 24	21.7 $\pm$ 2.5	>100 000	>100 000
28	209 $\pm$ 50	>100 000	520 $\pm$ 31	>100 000	>100 000
29	397 $\pm$ 66	18100 $\pm$ 5850	267 $\pm$ 30	>100 000	>100 000
30	1200 $\pm$ 180	>100 000	>100 000	>100 000	>100 000
31	72.7 $\pm$ 8.9	>100 000	53.5 $\pm$ 9.4	>100 000	>100 000
32	1730 $\pm$ 250	>100 000	>100 000	>100 000	>100 000
33	>100 000	>100 000	>100 000	>100 000	>100 000
34	>100 000	>100 000	>100 000	>100 000	>100 000
35	>100 000	>100 000	2150 $\pm$ 340	>100 000	>100 000
36	380 $\pm$ 110	1690 $\pm$ 240	823 $\pm$ 215	>100 000	>100 000
37	5.6 $\pm$ 0.4	8.0 $\pm$ 0.9	6.1 $\pm$ 0.6	>100 000	>100 000

<sup>a</sup> *o*-NPA was used as a substrate for the CEs, AcTCh for hAcChE, and BuTCh for hBuChE.**Table 5.**  $K_i$  Values for the Inhibition of hiCE, hCE1, rCE, hAcChE, and hBuChE for Compounds with Structural Similarity to Benzil<sup>a</sup>

compd	hiCE $K_i \pm SE$ (nM)	hCE1 $K_i \pm SE$ (nM)	rCE $K_i \pm SE$ (nM)	hAcChE $K_i \pm SE$ (nM)	hBuChE $K_i \pm SE$ (nM)
2	1840 $\pm$ 260	5270 $\pm$ 1730	4930 $\pm$ 1320	>100 000	>100 000
3	>100 000	>100 000	>100 000	>100 000	>100 000
4	>100 000	>100 000	>100 000	>100 000	>100 000
5	>100 000	26000 $\pm$ 1880	3950 $\pm$ 970	>100 000	>100 000
6	2220 $\pm$ 460	7250 $\pm$ 2370	>100 000	>100 000	>100 000
7	>100 000	>100 000	>100 000	>100 000	>100 000
38	>100 000	>100 000	13900 $\pm$ 2430	>100 000	>100 000
39	>100 000	>100 000	>100 000	>100 000	>100 000
40	>100 000	>100 000	>100 000	>100 000	>100 000
41	>100 000	>100 000	>100 000	>100 000	>100 000
42	>100 000	15300 $\pm$ 3380	>100 000	>100 000	>100 000
43	>100 000	>100 000	>100 000	>100 000	>100 000
44	>100 000	>100 000	>100 000	>100 000	>100 000
45	>100 000	>100 000	15700 $\pm$ 7960	>100 000	>100 000
46	>100 000	>100 000	>100 000	>100 000	>100 000
47	>100 000	16900 $\pm$ 2420	>100 000	>100 000	>100 000
48	>100 000	>100 000	>100 000	>100 000	>100 000
49	>100 000	>100 000	>100 000	>100 000	>100 000
50	>100 000	>100 000	>100 000	>100 000	>100 000
51	>100 000	>100 000	>100 000	>100 000	>100 000
52	>100 000	>100 000	>100 000	>100 000	>100 000
53	>100 000	>100 000	>100 000	955 $\pm$ 378	2050 $\pm$ 650
54	1350 $\pm$ 360	88.6 $\pm$ 6.2	736 $\pm$ 58	>100 000	>100 000
55	875 $\pm$ 103	5440 $\pm$ 900	1035 $\pm$ 105	1670 $\pm$ 520	3200 $\pm$ 780
56	57.4 $\pm$ 15	83.9 $\pm$ 41	54.8 $\pm$ 13	163 $\pm$ 50	268 $\pm$ 75
57	>100 000	>100 000	>100 000	>100 000	>100 000
58	>100 000	>100 000	>100 000	>100 000	>100 000
59	>100 000	>100 000	>100 000	>100 000	>100 000
60	>100 000	>100 000	>100 000	>100 000	>100 000
61	>100 000	>100 000	>100 000	>100 000	>100 000

<sup>a</sup> *o*-NPA was used as a substrate for the CEs, AcTCh for hAcChE, and BuTCh for hBuChE.

demonstrated no inhibition of hAcChE or hBuChE at concentrations up to 100  $\mu$ M. This is despite the fact that hAcChE and hBuChE are highly homologous to

CEs, both at the amino acid and structural level. While numerous inhibitors of the former enzymes have been identified, selective inhibitors of CEs have remained

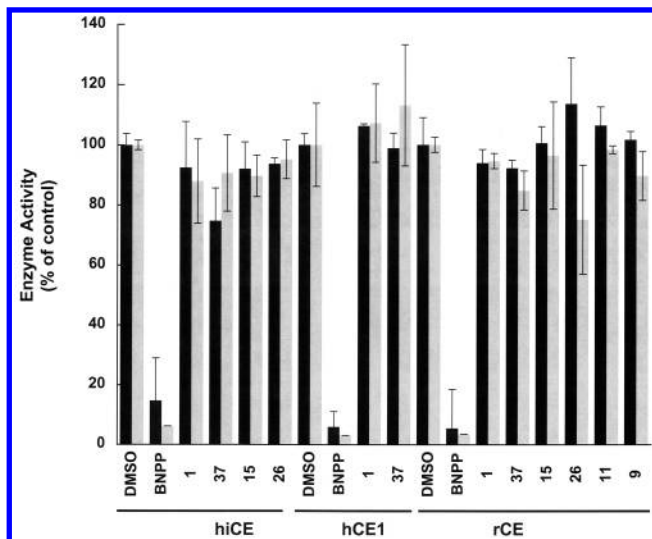


**Figure 1.** Lack of irreversible inhibition by benzil and selected analogues. Enzymes were incubated with 1  $\mu$ M inhibitor for either 1 h (black bars) or 24 h (gray bars) prior to CE enzyme activity analyses using *o*-NPA as a substrate. Data are presented as percent of enzyme activity remaining compared to enzyme treated with DMSO alone. Irreversible inhibition was only observed with the control compound BNPP.

elusive. This article represents the first report detailing the analysis of CE inhibition by 31 benzil analogues and 3D-QSAR studies assessing the contribution of substituents within the benzene rings toward inhibitory activity.

Analysis of a series of structurally similar analogues of benzil (Table 1) indicated that displacement of the 1,2-dione to the 1,3-derivative (1,3-diphenylpropane-1,3-dione, **5**) resulted in loss of enzyme inhibition. This suggested that the benzil compounds act as ester mimics. This is further exemplified by the fact that benzophenone inhibits none of the enzymes tested. Similarly, both hydroxyl forms of the benzil analogues (i.e., benzoin (**6**) and 1,2-diphenylethane-1,2-diol (**7**)) were poor inhibitors, again indicating that the dione is necessary for the inhibition of CE-mediated catalysis. From these studies, we conclude that for efficient selective inhibition of CEs, the following components are required: (1) the 1,2-dione moiety, (2) aromatic (or potentially highly hydrophobic) domains immediately adjacent to the dione, and (3) substitutions within the aromatic rings that do not impede access of the inhibitor

**Table 6.** Correlation Coefficients for QSAR Models

enzyme	observed vs predicted $K_i$ values ( $r^2$ )	cross-correlation coefficient ( $q^2$ )	$q^2/r^2$
hiCE	0.919	0.900	0.979
hCE1	0.925	0.900	0.973
rCE	0.923	0.900	0.975

to the enzyme active site.<sup>10</sup> Additionally, since the catalytic amino acids present within mammalian CEs are buried at the bottom of a long hydrophobic gorge,<sup>6–8</sup> it is likely that localization of the inhibitor in this domain is enhanced by the aromatic benzene rings present in the benzil analogues.<sup>10,38</sup> This concept was exemplified by compounds **2** and **3** (Table 1), where replacement of the benzene ring with methyl groups significantly reduced inhibitory activity.

Examination of the curve fits for the enzyme inhibition data indicated that in most cases  $\beta = 1$ ; i.e., there was no change in the rate of enzyme substrate complex decomposition in the presence of inhibitor.<sup>22</sup> In addition, the observed  $\alpha$  values were routinely greater than 1000 but less than  $\infty$ , indicating that the inhibitors acted in a partially competitive fashion toward CEs. These results suggest that the compounds only partially hinder binding of the substrate to enzyme.<sup>22</sup> Therefore, these compounds do not act in a strictly competitive manner; but since the 1,2-dione is structurally similar to the ester chemotype, it seems likely that the competitive component of the inhibition is due to the presence of the carbonyl functions within the molecule. This hypothesis is consistent with the data presented in Figure 1, showing that benzil was not an irreversible inhibitor of CEs. Since the initial step in substrate hydrolysis by CEs involves nucleophilic attack of the active site serine toward the carbonyl carbon, we propose that the reverse reaction can readily occur, liberating the free enzyme and benzil (Figure 4). Elimination of benzaldehyde in the second stage of the reaction would be energetically less favored compared to the re-formation of the carbonyl group, and hence, hydrolysis does not occur. Therefore, nonproductive cycling of the enzyme would occur in the presence of benzil-based inhibitors. Such a mechanism is consistent with the kinetic data.

Detailed examination of the 3D-QSAR models obtained using Quasar 4.0 allowed us to explain the large differences in inhibitory activity of some of the analogues. For example, the asymmetric distribution of

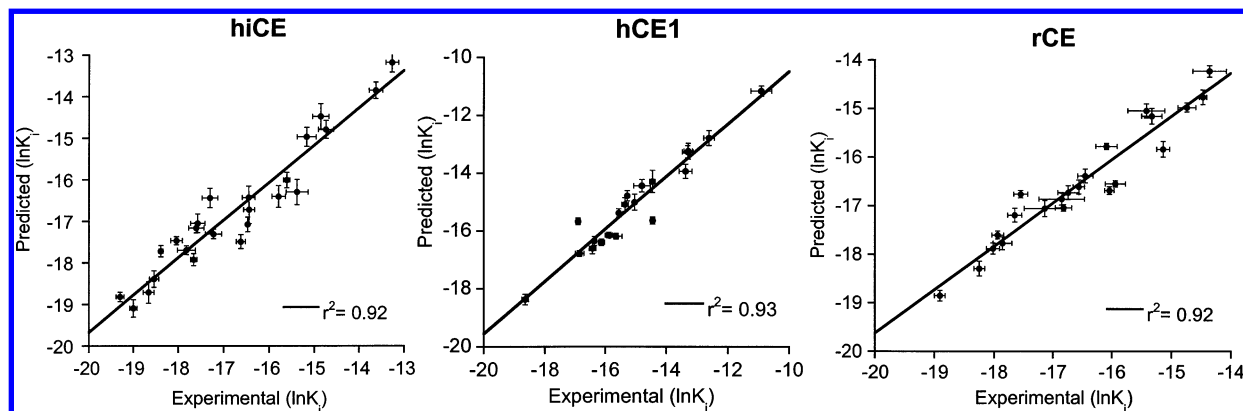


**Figure 2.** Graphs of experimental versus predicted  $K_i$  values for the benzil-based inhibitors as determined using the QSAR model for each protein. Predicted  $K_i$  values were obtained using the Quasar 4.0 program, and  $r^2$  values for the curve fits are indicated.



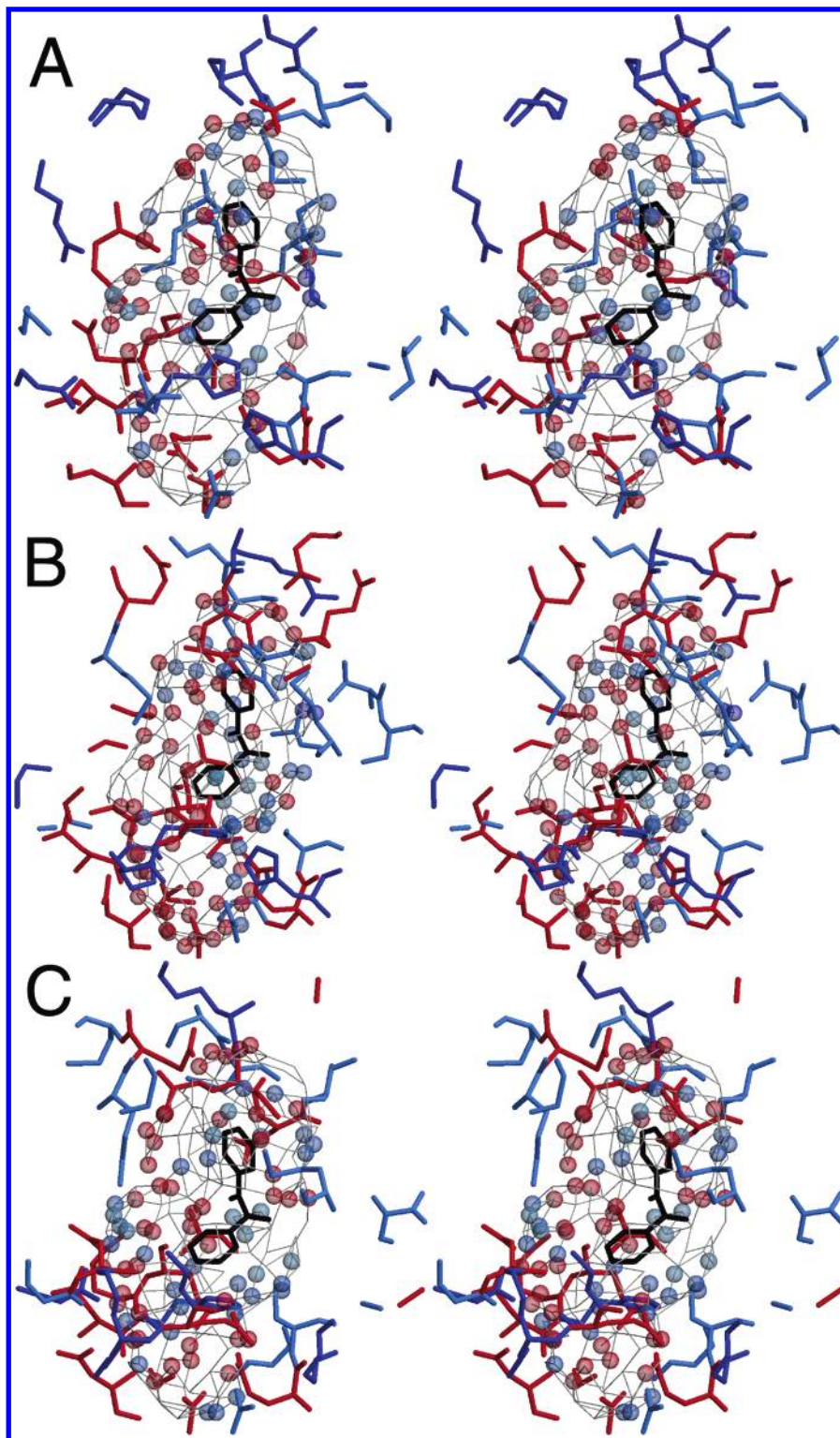


**Figure 3.** Pseudoreceptor site models for the benzil binding sites of the CEs. Stereomages for hiCE (A), hCE1 (B), and rCE (C) are shown. The model is represented by gray grid lines around a benzil molecule (black). His, Lys, and Arg residues are shown as blue, while Asp and Glu are indicated in red. Gln and Asn are depicted in light-blue. Those vertexes having charge are shown as transparent spheres. Increasing charge from  $+0.1e$  to  $+0.5e$  is represented by increasingly blue spheres, whereas decreasing charge from  $-0.1e$  to  $-0.5e$  is represented by increasingly red spheres ( $e$  is the charge of the proton).

anionic charges in the hCE1 model suggests that the lack of inhibition of hCE1 by 1,2-bis(5-bromo-2-hydroxyphenyl)ethane-1,2-dione (**31**) is due to the juxtaposition of the bromine atom next to anionic amino acid residues Glu<sup>334</sup> and Asp<sup>447</sup>. This interaction would not be favored and would decrease the affinity of this compound for the active site and hence increase the  $K_i$  value ( $>100$

$\mu\text{M}$ ). Likewise, the activity of the 4,4'-difluorobenzil and 4,4'-dibromobenzil analogues (compounds **8** and **11**, respectively) toward rCE may be due to favorable interaction of the halogen atoms with Lys<sup>292</sup> and Gln<sup>341</sup> near the gorge opening and with Arg<sup>439</sup> and Asn<sup>83</sup> near the gorge floor. These residues are displaced and/or absent in the hCE1 and hiCE models. On the basis of



**Table 7.**  $K_i$  Values for the Inhibition of hiCE, hCE1, and rCE for Selected Benzil-Based Inhibitors Using *o*-NPA, 4-MUA, or CPT-11 as Substrates

compd	$K_i \pm \text{SE}$ (nM) for the indicated substrate with the respective enzyme							
	hiCE			hCE1 <sup>a</sup>		rCE		
	<i>o</i> -NPA	4-MUA	CPT-11	<i>o</i> -NPA	4-MUA	<i>o</i> -NPA	4-MUA	CPT-11
benzil (1)	14.7 $\pm$ 1.9	24.0 $\pm$ 3.6	175 $\pm$ 29	45.1 $\pm$ 32	6.9 $\pm$ 0.4	103 $\pm$ 19	13.6 $\pm$ 0.9	185 $\pm$ 68
<b>9</b>	106 $\pm$ 22	27.5 $\pm$ 2.9	>100 000	182 $\pm$ 21	1.6 $\pm$ 0.2	9.5 $\pm$ 1.5	1.3 $\pm$ 0.1	43.0 $\pm$ 25
<b>11</b>	>100 000	18.6 $\pm$ 3.6	>100 000	>100 000	0.029 $\pm$ 0.008	4.1 $\pm$ 0.5	0.17 $\pm$ 0.04	25.0 $\pm$ 23
<b>15</b>	18.2 $\pm$ 3.6	29.7 $\pm$ 4.4	169 $\pm$ 49	47.4 $\pm$ 6.8	5.4 $\pm$ 0.5	23.9 $\pm$ 2.9	1.7 $\pm$ 0.1	52.5 $\pm$ 18
<b>19</b>	4.1 $\pm$ 0.4	3.2 $\pm$ 0.4	91.9 $\pm$ 26	99.1 $\pm$ 10	18.8 $\pm$ 2.7	108 $\pm$ 8.8	4.4 $\pm$ 1.1	240 $\pm$ 19
<b>26</b>	7.9 $\pm$ 0.9	4.4 $\pm$ 0.7	33.8 $\pm$ 14	295 $\pm$ 9.6	7.5 $\pm$ 1.5	11.9 $\pm$ 1.1	4.0 $\pm$ 0.2	24.1 $\pm$ 5.1
<b>37</b>	5.6 $\pm$ 0.4	9.8 $\pm$ 0.9	39.1 $\pm$ 19	8.0 $\pm$ 0.9	2.1 $\pm$ 0.1	6.1 $\pm$ 0.6	2.1 $\pm$ 0.1	14.1 $\pm$ 4.6

<sup>a</sup>  $K_i$  values were not calculated for CPT-11 with hCE1 because this drug is a very poor substrate for this enzyme.

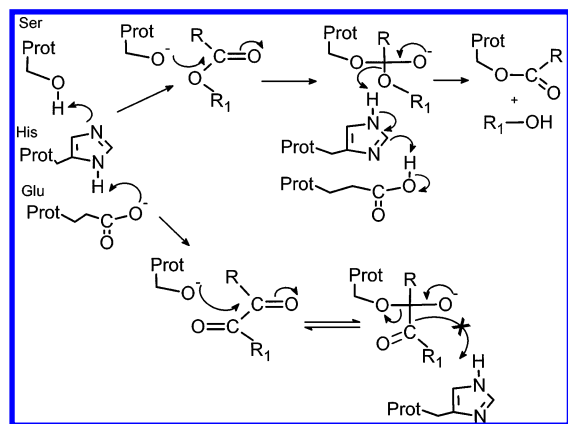


**Figure 4.** Potential mechanism of CE inhibition by benzil. In the upper reaction, the initial stages of the hydrolysis of an ester  $\text{RCOOR}_1$  are shown. Removal of the proton on the histidine (His) by the glutamic acid (Glu) results in proton transfer from the active site serine (Ser). The resulting nucleophile attacks the carbonyl carbon to yield a tetrahedral intermediate that undergoes a reverse reaction with cleavage of the ester bond to liberate the alcohol ( $\text{R}_1\text{OH}$ ). Subsequent hydrolysis to produce the carboxylic acid is achieved using water as a nucleophile (not shown). In the lower reaction, the interaction of the serine nucleophile with a benzil ( $\text{RCOCOR}_1$ ) is shown. The initial stage of the reaction is similar to that seen with the ester; however, release of the aldehyde does not occur (as indicated by the X) presumably because of the increased strength of the C–C bond as opposed to the C–O bond. Hence, repetitive reaction cycling of the catalytic amino acid residues with the benzil probably accounts for the inhibition of the enzyme.

these models, the design and synthesis of novel benzil analogues that demonstrate increased potency and selectivity for the different CEs are currently underway.

Since benzil and its analogues acted in a partially competitive fashion against the mammalian CEs, the  $K_i$  values for these inhibitors will depend on the  $K_m$  of the substrate for the enzyme.<sup>22</sup> Therefore, the potential existed for the benzils described here to be poor CE inhibitors with ester substrates other than *o*-NPA that was used for the initial screen. To determine if this was the case, we assessed the ability of a panel of benzil analogues to inhibit the metabolism of structurally unrelated esters. These included the highly effective anticancer agent CPT-11 and the simple fluorogenic substrate 4-MUA. As indicated in Table 7, selected benzil analogues effectively inhibited hiCE, hCE1, and rCE with these alternative substrates. While differences in levels of inhibition were observed among the three substrates, as would be expected for molecules that

acted in a competitive fashion, it is apparent that the benzils are potent inhibitors of mammalian CEs.

In some instances, we observed dramatic differences in the ability of certain analogues to inhibit the CEs with different substrates. For example, 4,4'-dibromobenzil (**11**) inhibited 4-MUA production from hiCE with a  $K_i$  value of 18.6 nM; yet this same compound did not inhibit the metabolism of *o*-NPA or CPT-11 (Table 7). Conversely 4,4'-dichlorobenzil (**9**) did not inhibit CPT-11 hydrolysis by hiCE but yielded  $K_i$  values of 106 and 27.5 nM when using *o*-NPA or 4-MUA as substrates, respectively. While we have not examined the QSAR models for these alternative substrates, such studies might reveal nuances within the active sites that account for the difference in the levels of enzyme inhibition. Such experiments are currently underway.

Overall, this article describes the selective inhibition of mammalian CEs by aromatic ethane-1,2-diones. Compounds with  $K_i$  values as low as 30 pM have been observed for the substrate 4-MUA. These inhibitors do not inhibit human AcChE and BuChE at concentrations up to 100  $\mu\text{M}$ , suggesting that some of the analogues represent useful lead compounds for modulating the activity of CEs in clinical applications. We are currently pursuing the use of benzil and its analogues for the modulation of esterified drug metabolism in vivo.

**Acknowledgment.** We thank Dr. J. P. McGovern for the gift of CPT-11. This work was supported in part by an NIH Cancer Center Core Grant P30 CA-21765 and by the American Lebanese Syrian Associated Charities.

## Appendix

**Abbreviations.** AcChE, acetylcholinesterase; AcTCh, acetylthiocholine; BNPP, bis(4-nitrophenyl) phosphate; BuChE, butyrylcholinesterase; BuTCh, butyrylthiocholine; CE, carboxylesterase; CPT-11, irinotecan, 7-ethyl-10-[4-(1-piperidino)-1-piperidino]carbonyloxycamptothecin; hAcChE, human AcChE; hBuChE, human BuChE; hCE1, human carboxylesterase 1; hCE2, human carboxylesterase 2; hiCE, human intestinal carboxylesterase; HPLC, high-performance liquid chromatography; 4-MUA, 4-methylumbelliferone acetate; *o*-NP, *o*-nitrophenol; *o*-NPA, *o*-nitrophenyl acetate;  $q^2$ , cross-validated correlation coefficients; QSAR, quantitative structure–activity relationship; rCE, rabbit liver carboxylesterase; SN-38, 7-ethyl-10-hydroxycamptothecin; TFK, trifluoroketones; TRAP, target-related affinity profiling.

**Supporting Information Available:** Elemental analysis results for compounds **9**, **12**, and **13**. This material is available free of charge via the Internet at <http://pubs.acs.org>.

## References

- Cashman, J.; Perroti, B.; Berkman, C.; Lin, J. Pharmacokinetics and molecular detoxification. *Environ. Health Perspect.* **1996**, *104*, 23–40.
- Kamendulis, L. M.; Brzezinski, M. R.; Pindel, E. V.; Bosron, W. F.; Dean, R. A. Metabolism of cocaine and heroin is catalyzed by the same human liver carboxylesterases. *J. Pharmacol. Exp. Ther.* **1996**, *279*, 713–717.
- Khanna, R.; Morton, C. L.; Danks, M. K.; Potter, P. M. Proficient metabolism of CPT-11 by a human intestinal carboxylesterase. *Cancer Res.* **2000**, *60*, 4725–4728.
- Redinbo, M. R.; Bencharit, S.; Potter, P. M. Human carboxylesterase 1: from drug metabolism to drug discovery. *Biochem. Soc. Trans.* **2003**, *31*, 620–624.
- Maxwell, D. M.; Brecht, K. M. Carboxylesterase: specificity and spontaneous reactivation of an endogenous scavenger for organophosphorus compounds. *J. Appl. Toxicol.* **2001**, *21*, S103–S107.
- Bencharit, S.; Morton, C. L.; Howard-Williams, E. L.; Danks, M. K.; Potter, P. M.; Redinbo, M. R. Structural insights into CPT-11 activation by mammalian carboxylesterases. *Nat. Struct. Biol.* **2002**, *9*, 337–342.
- Bencharit, S.; Morton, C. L.; Hyatt, J. L.; Kuhn, P.; Danks, M. K.; Potter, P. M.; Redinbo, M. R. Crystal structure of human carboxylesterase 1 complexed with the Alzheimer's drug tacrine. From binding promiscuity to selective inhibition. *Chem. Biol.* **2003**, *10*, 341–349.
- Bencharit, S.; Morton, C. L.; Xue, Y.; Potter, P. M.; Redinbo, M. R. Structural basis of heroin and cocaine metabolism by a promiscuous human drug-processing enzyme. *Nat. Struct. Biol.* **2003**, *10*, 349–356.
- Danks, M. K.; Morton, C. L.; Krull, E. J.; Cheshire, P. J.; Richmond, L. B.; Naeve, C. W.; Pawlik, C. A.; Houghton, P. J.; Potter, P. M. Comparison of activation of CPT-11 by rabbit and human carboxylesterases for use in enzyme/prodrug therapy. *Clin. Cancer Res.* **1999**, *5*, 917–924.
- Wadkins, R. M.; Morton, C. L.; Weeks, J. K.; Oliver, L.; Wierdl, M.; Danks, M. K.; Potter, P. M. Structural constraints affect the metabolism of 7-ethyl-10-[4-(1-piperidino)-1-piperidinol]carbonyloxycamptothecin (CPT-11) by carboxylesterases. *Mol. Pharmacol.* **2001**, *60*, 355–362.
- Wheelock, C. E.; Severson, T. F.; Hammock, B. D. Synthesis of new carboxylesterase inhibitors and evaluation of potency and water solubility. *Chem. Res. Toxicol.* **2001**, *14*, 1563–1572.
- Wheelock, C. E.; Colvin, M. E.; Uemura, I.; Olmstead, M. M.; Sanborn, J. R.; Nakagawa, Y.; Jones, A. D.; Hammock, B. D. Use of ab initio calculations to predict the biological potency of carboxylesterase inhibitors. *J. Med. Chem.* **2002**, *45*, 5576–5593.
- Molinoff, P. B.; Ruddon, R. W. In *Goodman & Gilman's the Pharmacological Basis of Therapeutics*; Hardman, J. G., Limbird, L. E., Eds.; McGraw-Hill: New York, 1996; p 1905.
- Beroza, P.; Villar, H. O.; Wick, M. M.; Martin, G. R. Chemo-proteomics as a basis for post-genomic drug discovery. *Drug Discovery Today* **2002**, *7*, 807–814.
- Dixon, S. L.; Villar, H. O. Bioactive diversity and screening library selection via affinity fingerprinting. *J. Chem. Inf. Comput. Sci.* **1998**, *38*, 1192–1203.
- Kauvar, L. M.; Higgins, D. L.; Villar, H. O.; Sportsman, J. R.; Engqvist-Goldstein, A.; Bukar, R.; Bauer, K. E.; Dilley, H.; Rocke, D. M. Predicting ligand binding to proteins by affinity fingerprinting. *Chem. Biol.* **1995**, *2*, 107–118.
- Morton, C. L.; Potter, P. M. Comparison of *Escherichia coli*, *Saccharomyces cerevisiae*, *Pichia pastoris*, *Spodoptera frugiperda*, and COS7 cells for recombinant gene expression: Application to a rabbit liver carboxylesterase. *Mol. Biotechnol.* **2000**, *16*, 193–202.
- Potter, P. M.; Pawlik, C. A.; Morton, C. L.; Naeve, C. W.; Danks, M. K. Isolation and partial characterization of a cDNA encoding a rabbit liver carboxylesterase that activates the prodrug Irinotecan (CPT-11). *Cancer Res.* **1998**, *58*, 2646–2651.
- Munger, J. S.; Shi, G. P.; Mark, E. A.; Chin, D. T.; Gerard, C.; Chapman, H. A. A serine esterase released by human alveolar macrophages is closely related to liver microsomal carboxylesterases. *J. Biol. Chem.* **1991**, *266*, 18832–18838.
- Schwer, H.; Langmann, T.; Daig, R.; Becker, A.; Aslanidis, C.; Schmitz, G. Molecular cloning and characterization of a novel putative carboxylesterase, present in human intestine and liver. *Biochem. Biophys. Res. Commun.* **1997**, *233*, 117–120.
- Beaufay, H.; Amar-Costesec, A.; Feytmans, E.; Thines-Sempoux, D.; Wibó, M.; Robbi, M.; Berthet, J. Analytical study of microsomes and isolated subcellular membranes from rat liver. I. Biochemical methods. *J. Cell Biol.* **1974**, *61*, 188–200.
- Webb, J. L. *Enzyme and Metabolic Inhibitors. General Principles of Inhibition*; Academic Press, Inc.: New York, 1963; Vol. 1.
- Akaike, H. Information theory and an extension of the maximum likelihood principle. In *2nd International Symposium on Information Theory*, Budapest, Hungary, 1973; Petrov, B. N., Csaki, F., Eds.; Akademiai Kiado: Budapest, Hungary, 1973; pp 267–281.
- Akaike, H. A new look at the statistical model identification. *IEEE Trans. Autom. Control* **1974**, *AC-19*, 716–723.
- Ellman, G. L.; Courtney, K. D.; Anders, V.; Featherstone, R. M. A new and rapid colorimetric determination of acetylcholinesterase activity. *Biochem. Pharmacol.* **1961**, *7*, 88–95.
- Doctor, B. P.; Toker, L.; Roth, E.; Silman, I. Microtiter assay for acetylcholinesterase. *Anal. Biochem.* **1987**, *166*, 399–403.
- Morton, C. L.; Wadkins, R. M.; Danks, M. K.; Potter, P. M. CPT-11 is a potent inhibitor of acetylcholinesterase but is rapidly catalyzed to SN-38 by butyrylcholinesterase. *Cancer Res.* **1999**, *59*, 1458–1463.
- Wadkins, R. M.; Potter, P. M.; Vladu, B.; Marty, J.; Mangold, G.; Weitman, S.; Manikumar, G.; Wani, M. C.; Wall, M. E.; Von Hoff, D. D. Water soluble 20(S)-glycinate esters of 10,11-methylenedioxycamptothecins are highly active against human breast cancer xenografts. *Cancer Res.* **1999**, *59*, 3424–3428.
- Mohrig, J. R.; Hammond, C. N.; Schatz, P. F.; Morrill, T. C. Thiamine-catalyzed benzoin condensation. In *Modern Projects and Experiments in Organic Chemistry: Miniscale and Williamson Microscale*; W. H. Freeman & Co.: New York, 2003; pp 367–368.
- Weiss, M.; Appel, M. The catalytic oxidation of benzoin to benzil. *J. Am. Chem. Soc.* **1948**, *70*, 3666–3667.
- Vedani, A.; Dobler, M. 5D-QSAR: the key for simulating induced fit? *J. Med. Chem.* **2002**, *45*, 2139–2149.
- Vedani, A.; Dobler, M. Multidimensional QSAR: Moving from three- to five-dimensional concepts. *Quant. Struct.-Act. Relat.* **2002**, *21*, 382–390.
- Jakalian, A.; Jack, D. B.; Bayly, C. I. Fast, efficient generation of high-quality atomic charges. AM1-BCC model: II. Parameterization and validation. *J. Comput. Chem.* **2002**, *23*, 1623–1641.
- Stewart, J. J. MOPAC: a semiempirical molecular orbital program. *J. Comput.-Aided Mol. Des.* **1990**, *4*, 1–105.
- Kolev, T. M.; Stamboliyska, B. A. Vibrational spectra and structure of benzil and its 18O- and d10-labelled derivatives: a quantum chemical and experimental study. *Spectrochim. Acta, Part A* **2002**, *58*, 3127–3137.
- Guichard, S.; Morton, C. L.; Krull, E. J.; Stewart, C. F.; Danks, M. K.; Potter, P. M. Conversion of the CPT-11 metabolite APC to SN-38 by rabbit liver carboxylesterase. *Clin. Cancer Res.* **1998**, *4*, 3089–3094.
- Koehler, R. T.; Dixon, S. L.; Villar, H. O. LASSOO: a generalized directed diversity approach to the design and enrichment of chemical libraries. *J. Med. Chem.* **1999**, *42*, 4695–4704.
- Wadkins, R. M.; Hyatt, J. L.; Yoon, K. J.; Morton, C. L.; Lee, R. E.; Damodaran, K.; Beroza, P.; Danks, M. K.; Potter, P. M. Identification of novel selective human intestinal carboxylesterase inhibitors for the amelioration of irinotecan-induced diarrhea: Synthesis, quantitative structure–activity relationship analysis, and biological activity. *Mol. Pharmacol.* **2004**, *65*, 1336–1343.
- Lundstedt, T.; Seifert, E.; Abramo, L.; Thelin, B.; Nystrom, A.; Pettersen, J.; Bergman, B. Experimental design and optimization. *Chemom. Intell. Lab. Syst.* **1998**, *42*, 3–40.